symmetry

MDPI

Article

Optimal Location and Sizing of PV Sources in DC Networks for Minimizing Greenhouse Emissions in Diesel Generators

Oscar Danilo Montoya [1,2], Luis Fernando Grisales-Noreña [3], Walter Gil-González [2], Gerardo Alcalá [4] and Quetzalcoatl Hernandez-Escobedo [5,*]

1 Facultad de Ingeniería, Universidad Distrital Francisco José de Caldas, Carrera 7 No. 40B - 53, Bogotá D.C 11021, Colombia; o.d.montoyagiraldo@ieee.org or omontoya@utb.edu.co
2 Laboratorio Inteligente de Energía, Universidad Tecnológica de Bolívar, Km 1 vía Turbaco, Cartagena 131001, Colombia; wjgil@utp.edu.co
3 Departamento de Electromecánica y Mecratrónica, Instituto Tecnológico Metropolitano, Medellín 050012, Colombia; luisgrisales@itm.edu.co
4 Centro de Investigación en Recursos Energéticos y Sustentables, Universidad Veracruzana, Coatzacoalcos, Veracruz 96535, Mexico; galcala@uv.mx
5 Escuela Nacional de Estudios Superiores Juriquilla, UNAM, Queretaro 76230, Mexico
* Correspondence: qhernandez@unam.mx

Received: 27 December 2019; Accepted: 10 February 2020; Published: 24 February 2020

Abstract: This paper addresses the problem of the optimal location and sizing of photovoltaic (PV) sources in direct current (DC) electrical networks considering time-varying load and renewable generation curves. To represent this problem, a mixed-integer nonlinear programming (MINLP) model is developed. The main idea of including PV sources in the DC grid is minimizing the total greenhouse emissions produced by diesel generators in isolated areas. An artificial neural network is employed for short-term forecasting to deal with uncertainties in the PV power generation. The general algebraic modeling system (GAMS) package is employed to solve the MINLP model by using the CONOPT solver that works with mixed and integer variables. Numerical results demonstrate important reductions of harmful gas emissions to the atmosphere when PV sources are optimally integrated (size and location) to the DC grid.

Keywords: artificial neural networks; diesel generation; direct current networks; greenhouse emissions; numerical optimization; mixed-integer nonlinear programming photovoltaic plants

1. Introduction

Recent deployments of power electronics have allowed the positive advancement and development of efficient renewable energy interfaces for wind and photovoltaic plants [1–3], and the large-scale usage of energy storage systems, such as batteries [4–6], supercapacitors [7,8], superconductors [3,9,10] and flywheels [11,12]. These devices can be integrated into the power system using different interface technologies; i.e., to operate in the classical alternating current (AC) or direct current (DC) grids [3,13]. The selection of the grid operative condition plays an important role in the quality of the electrical service provided to the end-users. In the case of AC grids, it is required to maintain sinusoidal voltages with adequate form (power quality criteria); i.e., magnitude, frequency, power factor, harmonics, etc. [14–16]. These characteristics in AC networks make them more complex in comparison to DC networks, since these latter only require voltage control, and reactive power and frequency are nonexistent [17,18]. An additional advantage of using DC over AC technologies is their high efficiency in terms of power loss and voltage profiles [19]. These features can be added

to the fact that photovoltaic plants or some energy storage technologies (supercapacitors, batteries and superconducting coils) work directly in the DC paradigm [17,20], which can help to reduce the number of power interfaces to integrate these technologies in DC grids in comparison to their AC counterparts [21].

In specialized literature, DC networks have taken relevance regarding optimization and control applications [21]. In the case of optimization, multiple approaches based on semidefinite programming [4], second-order cone programming [20], sequential quadratics [22] and metaheuristics have been proposed to address optimal power flow problems [23]; additionally, some classical numerical methods can be found, such as Newton-Raphson [24], Gauss-Seidel [17] or successive approximations for power flow solutions [25]. In the case of control, the most conventional approaches focus on battery control [26], renewable energy integration [27] and dynamic stability based on passivity based-control [28,29], model predictive control [30,31] and sliding mode control [32,33].

These recent studies show that DC networks are promissory technologies that require extensive research for being successfully operated and also integrated and interconnected to the conventional AC power system [34,35]. In this paper, we deal with a classical and well-studied problem of optimal location and sizing of distributed generation in power systems. Nevertheless, we focus on direct current networks in isolated areas operated with diesel generators [36,37]. Although this problem has been widely studied in AC networks with metaheuristics, such as genetic algorithms [38], tabu search [39], harmonic search [40], krill-herd algorithm [41] and population based-learning methods [42], in conjunction with exact mixed-integer nonlinear programming methods [43,44], on the topic of DC networks there are only four references that address this problem. In [45] a semidefinite programming method was proposed for binary variable relaxation associated with the location of the generators; then, its binary structure was recovered with random hyperplanes; in [46] a sequential quadratic programming model with the same binary relaxation was proposed, and the binary nature of the problem was recovered with a heuristic search that defines the optimal location of the generators. The authors of [47] have addressed the issue of optimal location and sizing of distributed generators in DC networks from the metaheuristic point of view by using a classical genetic algorithm for their locations, in conjunction with their different optimal power flow methods based on particle swarm, black hole and continuous genetic optimizers. In [48], a mixed-integer nonlinear programming model was proposed to locate and size DGs in DC microgrids, using the general algebraic modeling system (GAMS) package for its solution. The common denominator of these approaches is the fact that load or renewable generation variations are not considered, since all of them only solve the problem for a unique hour time lapse. This cannot replicate the real behavior of electrical networks, especially when renewable energy resources are introduced.

To deal with renewable energy variations in the problem of optimal location and sizing of distributed generators in DC networks, here, we propose mixed-integer nonlinear programming for location and sizing of PV plants in DC networks to minimize the total pollution and greenhouse emissions released by diesel generators feeding isolated DC networks. The main contribution of our approach is based on a multiperiod optimization problem, including expected curves of PV generation and demand consumption focused on Colombian power system characteristics. To ensure that PV generation potential was well estimated, an artificial neural network with recursive connections was employed. To solve the proposed mixed-integer nonlinear programming (MINLP) model, we used the GAMS package with multiple nonlinear solvers to compare the results, as recommended in [44,48]. Numerical results confirm that the correct placement of PV plants helps via a significant reduction of pollutants released to the atmosphere by fossil fuels, which contributes positively to the responsible plans of energy consumption for future generations; i.e., making the power system more sustainable [6].

The remainder of this document is organized as follows: In Section 2 is presented the MINLP model for the problem of optimal location and sizing of PV generators in DC networks, for the reduction of greenhouse emissions with multiperiod structure. In Section 3 it the artificial neural

network employed to forecast the solar power generation is described. In Section 4 a GAMS example in a small DC network to solve the problem addressed in this paper is presented. In Section 5 the numerical simulation in a 21-nodes test feeder is shown to minimize pollutants produced by diesel generators with its corresponding analysis and discussion. In section 6 the main concluding remarks derived from this research are presented.

2. Mathematical Model

The problem of the optimal location of PV plants in DC networks considering load variations corresponds to a nonlinear, non-convex and non-differentiable optimization problem that combines discrete and continuous variables, which generates an MINLP problem [47]. The main interest in this formulation is to minimize the greenhouse emissions produced by diesel generators interconnected to DC rural (isolated) networks [48,49]. The complete mathematical model is presented below:

Objective function:

$$\min z = \sum_{t=1}^{T} \sum_{i=1}^{N} R_i^{ge} p_{i,t}^{cg} \Delta t, \tag{1}$$

where z are the total greenhouse emissions in pounds; R_i^{ge} is the rate of greenhouse emissions per kilowatt-hour; $p_{i,t}^{cg}$ is the total power generation in the conventional generators (diesel sources); and Δt is the period of time under analysis, typically $\Delta t = 1$ h. Note that N is the total number of nodes in the DC grid and T is the number of periods of time, N and T being the sizes of the sets of nodes $\mathcal{N}$ and periods of time $\mathcal{T}$, respectively.

Set of constraints:

$$p_{i,t}^{cg} + y_i^{pv} p_{i,t}^{pv,nom} - p_{i,t}^{d} = v_{i,t} \sum_{j=1}^{N} G_{ij} v_{j,t}, \qquad \forall \{i \in \mathcal{N}, t \in \mathcal{T}\} \tag{2}$$

$$i_{ij,t} = g_{ij} \left(v_{i,t} - v_{j,t}\right), \qquad \forall \{ij \in \mathcal{L}, t \in \mathcal{T}\} \tag{3}$$

$$p_{i,t}^{cg,\min} \leq p_{i,t}^{cg} \leq p_{i,t}^{cg,\max}, \qquad \forall \{i \in \mathcal{N}, t \in \mathcal{T}\} \tag{4}$$

$$-i_{ij}^{\max} \leq i_{ij,t} \leq i_{ij}^{\max}, \qquad \forall \{ij \in \mathcal{L}, t \in \mathcal{T}\} \tag{5}$$

$$v_i^{\min} \leq v_{i,t} \leq v_i^{\max}, \qquad \forall \{i \in \mathcal{N}, t \in \mathcal{T}\} \tag{6}$$

$$0 \leq y_i^{pv} \leq p_i^{pv,\max} x_i^{pv}, \qquad \forall \{i \in \mathcal{N},\} \tag{7}$$

$$\sum_{i=1}^{N} x_i^{pv} \leq NG_{pv}^{\max}, \tag{8}$$

where $p_{i,t}^{pv,nom}$ and $p_{i,t}^{d}$ are the nominal power injection of the PV generator and the power consumption in the node i during the period of time t; y_i^{pv} defines the size of the PV generator connected to the node i; $p_{i,t}^{pv,nom}$ is the nominal power of the PV generators, which is dependent on the solar forecasting in the zone of influence of the DC network; $v_{i,t}$ and $v_{j,t}$ represent the voltage value in the nodes i and j respectively during the time t; G_{ij} is the component of the conductance matrix that relates nodes i and j, whose value depends on the physical connections between nodes (i.e., it is dependent on the grid configuration); $i_{ij,t}$ represents the value of the current that flows between nodes i and j in the period time t, which depends on the conductor conductance named g_{ij}; $p_{i,t}^{cg,\min}$ and $p_{i,t}^{cg,\max}$ represent the minimum and maximum capabilities of power generation in the diesel generators connected at the node i in the period of time t; $p_i^{pv,\max}$ is the maximum nominal size of the PV source that can be connected in the node i; $i_{ij}^{\max}$ corresponds to the maximum current that can flow through the conductor that connects nodes i and j; $v_i^{\min}$ and $v_i^{\max}$ are the minimum and maximum voltage bounds allowed at each node; x_i^{pv} is a binary variable that defines whether a PV source is installed ($x_i^{pv} = 1$ if the PV source is installed and $x_i^{pv} = 0$ otherwise) at node i; $NG_{pv}^{\max}$ defines the maximum number of PV

generators available to be located into the grid. (The components G_{ij} and g_{ij} have the same magnitude; notwithstanding, these differ by sign, $g_{ij} = \frac{1}{r_{ij}}$ being positive; i.e., $G_{ij} = -g_{ij}$. r_{ij} is the resistance value of the conductor located between nodes i and j.)

The mathematical model defined from (1) to (8) has the following interpretation [22,50]: the objective function (1) quantifies the total greenhouse emissions produced by the diesel generators during their operation; in (2) is presented the power balance equation per node, which is typically known as power flow constraint, this being a non-affine constraint. Expression (3) shows the calculation of the current flow through ijth branch as a function of the voltage drop; in (4) is defined the box constraint related with the power capabilities in the diesel generators; in (5) the thermal bounds of the network conductors are presented in Amperes; meanwhile, (6) defines the voltage regulation bounds of the grid, which are defined by regulatory entities. Expression (7) determines the possibility of locating a PV generator in the network by defining its maximum ranks admissible for a generation. Finally, in (8) is presented the constraint associated with the maximum number of generators available for installation.

Note that the mathematical optimization model is complex to be solved, since it combines binary and integer variables, this model being an MINLP [45]. Additionally, the most complicated constraint is the power balance defined in (2), since it represents the hyperbolic relation between voltage and currents in electrical DC networks with constant power loads [51], which is a non-affine nonlinear constraint without convex properties.

Even though in specialized literature it has been reported, some approaches to solving this problem by decoupling it into a master-slave optimization problem with metaheuristics (i.e., genetic algorithms with particle swarm derived approaches [47]), no reports with the multiperiod structure (1)–(8) were found. For this reason, we are concentrating on the mathematical formulation and not on the solution technique. Since recent publications use the GAMS package and its large-scale nonlinear optimizers to solve similar problems [44,48], we decided to use the GAMS package in conjunction with the CONOPT solver as a solution strategy.

3. Solar Generation Forecasting

Planification of electrical networks that include renewable generators is a challenge, since it is necessary to consider their intermittency into the planning project. Due to that, in this research, we are interested in locating and sizing PV plants in DC networks to diminish greenhouse emissions produced by diesel generators for isolated areas, it being strictly necessary to know the PV potential in these areas. For this purpose, we consider that this electrical network is located in the Caribbean region in Colombia, and the solar power availability measured during a year is presented in Figure 1.

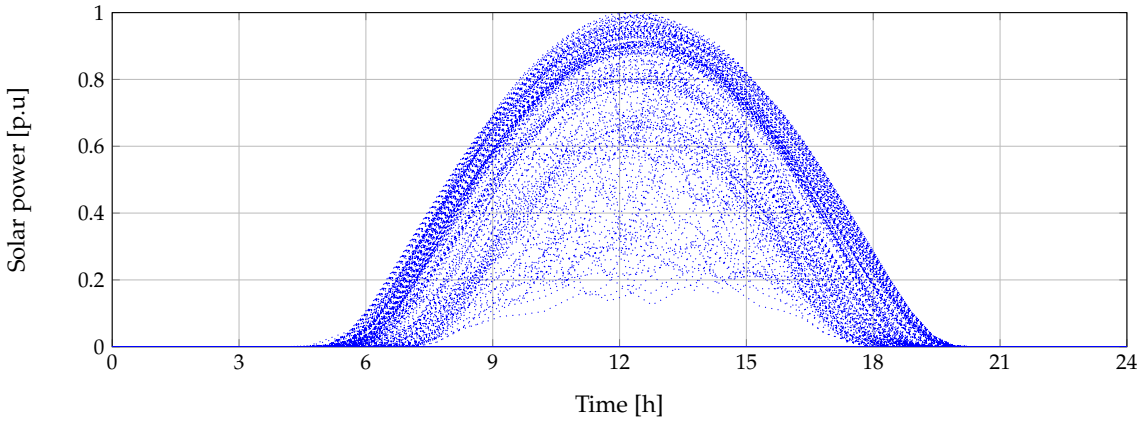

Figure 1. Historical data for solar prediction (adapted from [4,50]).

On the other hand, the uncertainty of primary sources for PV plants due to temperature and solar radiation produces a challenge for their optimal location and sizing. An improper location or sizing of PV plants can generate problems in the voltage profiles or cause transmission line overload and increase power loss [4]. Therefore, it is necessary to consider a methodology that takes into account the high variability of the temperature and solar radiation with the purpose of reducing the forecasting errors, and thus, avoiding problems that can be introduced due to incorrect location or sizing. For this purpose, we employ the methodology developed in [50], which uses an artificial neural network (ANN) in order to estimate the primary sources for PV plants adequately.

Artificial Neural Network

Artificial neural networks have been largely used to solve multiple problems in engineering, and are based on artificial intelligence [4]. They have a wide range of applications, from pattern classification and clustering, to optimization and prediction, among others [50]. Here the ANNs are used to predict the most probable temperature and solar radiation.

Typically, the ANNs go through three processes: training, adjusting and validating. There are multiples nonlinear learning rules to use in the training. We used the following rule to train the ANN:

$$y(t) = f\left(y(t-1), ..., y(t-n_y), x(t-1), ..., x(t-n_x)\right) \tag{9}$$

where x and y are input and output data, respectively. n_y and n_x are the last values of the prediction and the input data, respectively.

The ANN applied to solar radiation forecasting has been trained, adjusted and validated with 70%, 15% and 15% of the data, respectively. Additionally, two inputs (time and temperature), six delays and 18 hidden neurons have been implemented on the ANN. This was implemented in MATLAB R2019b employing *ntstool*. Figure 2 depicts its schematic implementation.

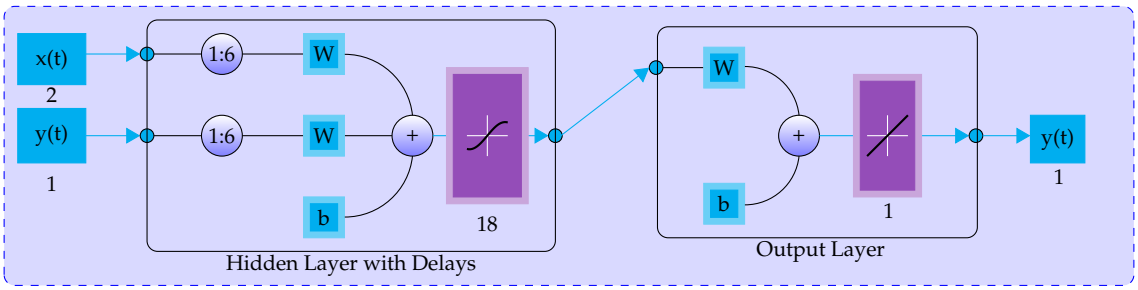

Figure 2. ANN scheme for solar radiation prediction [50].

The ANN scheme illustrated in Figure 2 contains a two-layer feedforward network. The first is the hidden layer that works with a sigmoid transfer function, while the second one is the output layer, which consists of a linear transfer function. The hidden layer uses delays to stores previous values of input $x(t)$ and output $y(t)$ data. W and b are weights and bias values in the training process of the proposed ANN, respectively. The output $y(t)$ in the output layer also applies rectified linear unit (ReLU) layer, which consists of

$$f(y) = \begin{cases} y, \ y \geq 0, \\ 0, \ y < 0. \end{cases} \tag{10}$$

The ReLU layer is used since in some cases the radiation estimation may be negative.

In the training process of the proposed ANN for solar forecasting the Levenberg–Marquardt algorithm was employed and it is available for the *ntstool* in MATLAB [52]. The main advantage of this training process in relation to classical Newton algorithm or Gauss-Newton algorithm is the rate

of convergence and its stability. More information about the Levenberg-Marquardt algorithm can be found in [53,54].

4. Optimization Strategy

The solution of the mathematical model described from (1) to (8) requires a methodology that works with mixed-integer variables [45]. In the specialized literature, two main approaches have been proposed to deal with MINLP models in power systems. One of them corresponds to the hybridization methods composed by master-slave stages with metaheuristics. Some of them are genetic algorithms [38], the particle swarm optimizer [42], tabu search algorithms [39] and krill-herd algorithms [41]. These methods decouple the problem of PV source location from sizing. The solutions of these problems are reached through iterative procedures; nevertheless, the optimal solution depends on the number of iterations defined, with the main disadvantage that it is not possible to find the same numerical solution each time that the methodology is evaluated [42]. Thus, statistical procedures are needed to determine their efficiencies [46]. The second focus is to solve MINLP models using gradient-based approaches embedded into branch and bound (B&B) methods, where the gradient searches solve the resulting nonlinear programming model, while the B&B guides the discrete search by defining the location of the PVs [43]. These approaches use nonlinear large-scale solvers available in optimization packages such as GAMS [6,44]. Here, due to the contribution of this paper being related to the presentation of the MINLP model to locate and size PV sources in DC grids for isolated areas to reduce greenhouse emissions by diesel generators, we solve the proposed mathematical model using the CONOPT solver available for GAMS.

As mentioned before, this solver works with gradient searches and B&B methods. In the first step, all the binary variables are relaxed to find the best possible solution; then, this relaxation is discretized to recover the nature of the binary variables in order to provide the optimal solution of the problem. It is important to mention that this optimization package has been successfully used in different problems, such as the optimal operation of batteries [6], optimal location of distributed generators in AC and DC grids [44], optimal design of osmotic power plants [55] and economic dispatch analysis [50,56]. Finally, Algorithm 1 resumes the necessary steps to solve the MINLP model defined from (1) to (8) [57].

Algorithm 1: Main steps for solving the proposed MINLP model in GAMS [57]

Select the test system characteristics;
Define the sets involved in the optimization model;
Define the scalars, parameters and matrices of the DC grid;
Define the variables and their bounds;
Define the name of the equations and build the mathematical model (1) to (8);
Determine the number of PV to be located;
Select the CONOPT solver in GAMS;
Define the variables of interest to be visualized;
Read and analyze the final results;

5. Test System and Numerical Validations

In this section, we present the test system structure and the output behavior of the PV forecasting used as input on the location and sizing process; in addition, all the simulation scenarios are defined and the numerical results are presented using the GAMS optimization package with its large-scale nonlinear solver CONOPT [44].

5.1. Test System

As the DC distribution system, we consider a 21-node test system with two slack (diesel) generators located at nodes 1 and 21, which support voltage profiles in the grid with 1.0 and 1.05 p.u,

respectively. The configuration of this test system is depicted in Figure 3 and the base values of this test system are 1 kV and 100 kW [4].

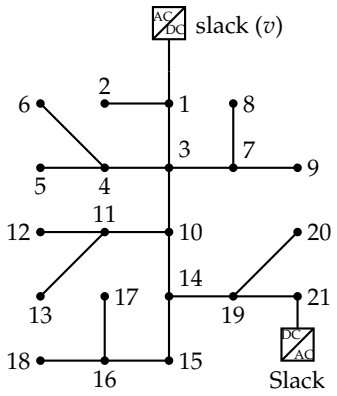

Figure 3. Electrical configuration for the 21-node test system.

Table 1 reports the numerical information of this test system, where its interpretation from left-to-right is as follows: Sending node, receiving node, branch resistance and power consumption at the receiving node. Note that in the case of the diesel generator located at node 21, there is a constant power consumption connected to its node.

Note that the total power consumption of this test feeder at the peak load is 554 kW.

Table 1. Electrical parameters of the 21-node test system.

Node i	Node j	R_{ij} [pu]	P_j [pu]	Node i	Node j	R_{ij} [pu]	P_j [pu]
1(slack)	2	0.0053	0.70	11	12	0.0079	0.68
1	3	0.0054	0.00	11	13	0.0078	0.10
3	4	0.0054	0.36	10	14	0.0083	0.00
4	5	0.0063	0.04	14	15	0.0065	0.22
4	6	0.0051	0.36	15	16	0.0064	0.23
3	7	0.0037	0.00	16	17	0.0074	0.43
7	8	0.0079	0.32	16	18	0.0081	0.34
7	9	0.0072	0.80	14	19	0.0078	0.09
3	10	0.0053	0.00	19	20	0.0084	0.21
10	11	0.0038	0.45	19	21(slack)	0.0082	-0.21

5.2. Objective Function and Daily Curves

To determine the number of greenhouse emissions by using diesel generators, we consider the information reported in [6]. In this reference the number of different greenhouse emissions caused by diesel generators with sizes smaller than 1 MW is presented. This information is reported in Table 2.

Table 2. Main gasses released by diesel generators with capacities lower than 1 MW.

Type of Emission	Chemical Symbol	Rank [lb/MWh]
Carbon dioxide	CO_2	1000–1700
Sulfur dioxide	SO_2	0.40–3.00
Nitrogen oxides	NO_x	10–41
Carbon monoxide	CO	0.40–9.00
Heavy particles	$PM-10$	0.40–3.00

Due to the most important emissions being carbon dioxide (CO_2), we select the average value in the rank, i.e., 1350 lb/MWh, to consider in the objective function. In the case of renewable generation prediction, in Table 3 a typical curve is reported for a sunny day in the Caribbean region in Colombia,

as is the prediction reached by the proposed ANN. (This information is presented numerically to guarantee that results can be reproduced in future research.) In addition, we include a curve for power consumption provided by a utility in Colombia. (The name of the utility is not provided due to confidential agreements.) Note that these curves are normalized to make them independent of the size of the PV source or the size of the utility [44,50].

Table 3. Real and predictive PV curves and load behavior during a typical sunny day in Colombia.

Period	Real [pu]	Forec. [pu]	Load [pu]	Period	Real [pu]	Forec. [pu]	Load [pu]
1	0.000	0.000	0.633	25	1.000	0.976	0.814
2	0.000	0.000	0.619	26	0.975	1.000	0.842
3	0.000	0.000	0.605	27	0.771	0.978	0.869
4	0.000	0.000	0.578	28	0.889	0.790	0.886
5	0.000	0.000	0.550	29	0.630	0.883	0.902
6	0.000	0.000	0.495	30	0.593	0.604	0.905
7	0.000	0.000	0.440	31	0.404	0.606	0.908
8	0.000	0.000	0.435	32	0.366	0.357	0.908
9	0.000	0.000	0.429	33	0.231	0.328	0.908
10	0.000	0.000	0.421	34	0.203	0.142	0.935
11	0.000	0.000	0.413	35	0.130	0.142	0.963
12	0.000	0.000	0.419	36	0.053	0.073	0.987
13	0.000	0.000	0.426	37	0.008	0.019	0.988
14	0.000	0.000	0.433	38	0.000	0.008	0.989
15	0.000	0.026	0.440	39	0.000	0.000	0.990
16	0.024	0.052	0.495	40	0.000	0.000	0.995
17	0.124	0.110	0.550	41	0.000	0.000	1.000
18	0.272	0.263	0.550	42	0.000	0.000	0.995
19	0.439	0.431	0.550	43	0.000	0.000	0.990
20	0.604	0.594	0.605	44	0.000	0.000	0.935
21	0.733	0.730	0.660	45	0.000	0.000	0.880
22	0.810	0.830	0.701	46	0.000	0.000	0.770
23	0.860	0.875	0.743	47	0.000	0.000	0.660
24	0.984	0.899	0.778	48	0.000	0.000	0.633

5.3. Simulation Scenarios

To evaluate our proposed mathematical model for optimal location and sizing of PV sources in DC grids, we consider that the size of these generators can be 60% of the total demand in the peak hour; i.e., 332.4 kW. In addition, we consider four simulation cases as follows: $\mathbf{S}_1$) as the base case of the test system without including PV sources, $\mathbf{S}_2$) as the location of one PV source, $\mathbf{S}_3$) as the location of two PV sources and $\mathbf{S}_4$) as the location of three PV sources inside of the DC system. The main idea of these scenarios is to evidence the effect of having a total PV installation capacity distributed in different quantities of injection depending on the simulation case.

5.4. Numerical Results

To solve the general MINLP model, which represents the problem of optimal location and sizing of DGs in DC systems, we employed the GAMS optimization package with different nonlinear solvers in a desktop computer with an INTEL(R) Core(TM) i5-3550 3.5-GHz processor and 8 GB of RAM running a 64-bit version of Windows 10 Home Single Language.

Table 4 reports the numerical results for all the simulation scenarios previously proposed. Note that in the first scenario, the daily greenhouse emissions of CO_2 are 13,428.912 pounds, and the minimum emissions occur in the fourth scenario with 10,878.190 pounds per day, which implies en equivalent reduction of 2550.722 pounds of emissions of CO_2 per day (18.99%). It is important to mention that after using the CONOPT solver for each simulation scenario, the total processing time to reach the optimal solution is lower than 20 s for all the cases. Still, it starts to increase from 6.224 s to 19.063 s (67.35%) depending on the number of PV sources that are considered in the scenario. It is

important to mention that the processing times of the ANN training process is not considered in the last column in Table 4, since this is an offline procedure that takes between 5 and 10 min depending on the size of the training set.

Table 4. Gas emissions for each simulation case.

Simulation Scenario	Objective Function [lb] (CO_2)	Processing Time [s]
$\mathbf{S}_1$	13,428.91	6.224
$\mathbf{S}_2$	11,027.19	11.001
$\mathbf{S}_3$	10,892.80	18.478
$\mathbf{S}_4$	10,878.18	19.063

Figure 4 presents the total daily reduction per day when a different number of PV sources are located and sized in the 21 nodes DC test feeder. This plot confirms that the best scenario corresponds to the case with three PV sources located inside the network; nevertheless, these bars confirm that the reduction of greenhouse emissions has a nonlinear behavior regarding the number of PV sources; i.e., the reduction tends to have a saturation of 19% approximately. This behavior obeys the fact that the PV sources only work during sunny hours, making it necessary to use diesel sources during the night.

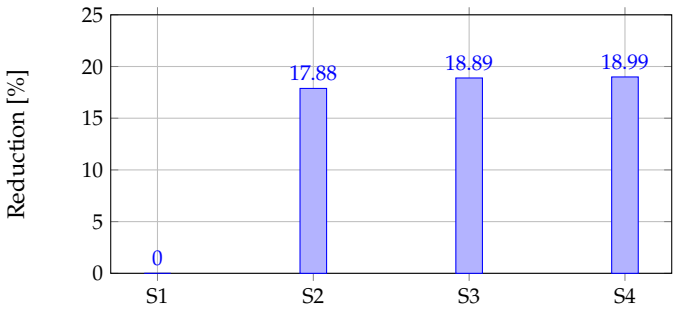

Figure 4. Total reductions in CO_2 emissions per day for each simulation scenario.

Table 5 reports the optimal location of the PV sources in each simulation scenario. These simulations show that the most attractive node to locate a PV source is the node 17, followed by nodes 19 and 12, respectively. In addition, for the third and fourth scenarios, it is important to observe that all the allowed penetration, i.e., 60% of the peak consumption, is used (divided) by the PV generators, while the second scenario only uses about 96.38% of this maximum capability. These results confirm the nonlinear relation between the number of sources available for location and their sizes regarding the minimization of the objective function, which implies that multiple simulations and scenarios need to be taken into account for the grid planner (i.e., utility) to determine its inversions.

Table 5. Optimal locations and sizes of the PV sources.

Simulation Scenario	Location [node]			Size [kW]			Total Penetration [kW]
$\mathbf{S}_1$	—	—	—	—	—	—	0
$\mathbf{S}_2$	17	—	—	320.37	—	—	320.372
$\mathbf{S}_3$	17	19	—	141.30	191.098	—	332.400
$\mathbf{S}_4$	12	17	19	91.33	101.582	139.485	332.400

Note that all the simulations were guaranteed through (5) to have all the currents flowing inside of the system be lower than 400 A; i.e., all the possible locations and sizes of the PV sources are feasible to be implemented since conductors of the grid can operate safely. In addition, when we considered the real daily curve reported in Table 3 with the locations and sizes of the PV sources reported in Table 5, it was found that the errors in the estimation of the objective function were lower than 1%,

which confirms that ANN are powerful tools for short-term forecasting of renewable energy resources, as reported in [50].

Figure 5 presents the behavior of the diesel generators during the day for all the simulated scenarios. Note that in the first scenario, they support all the power consumption in the DC grid (solid line in Figure 5a,b). Nevertheless, when PV generators are installed, the total generation in the diesel resources decreases significantly between hours 7 and 18; which clearly corresponds to the periods of time where PV sources can deliver their power to the grid (see dotted and dashed lines in Figure 5a,b).

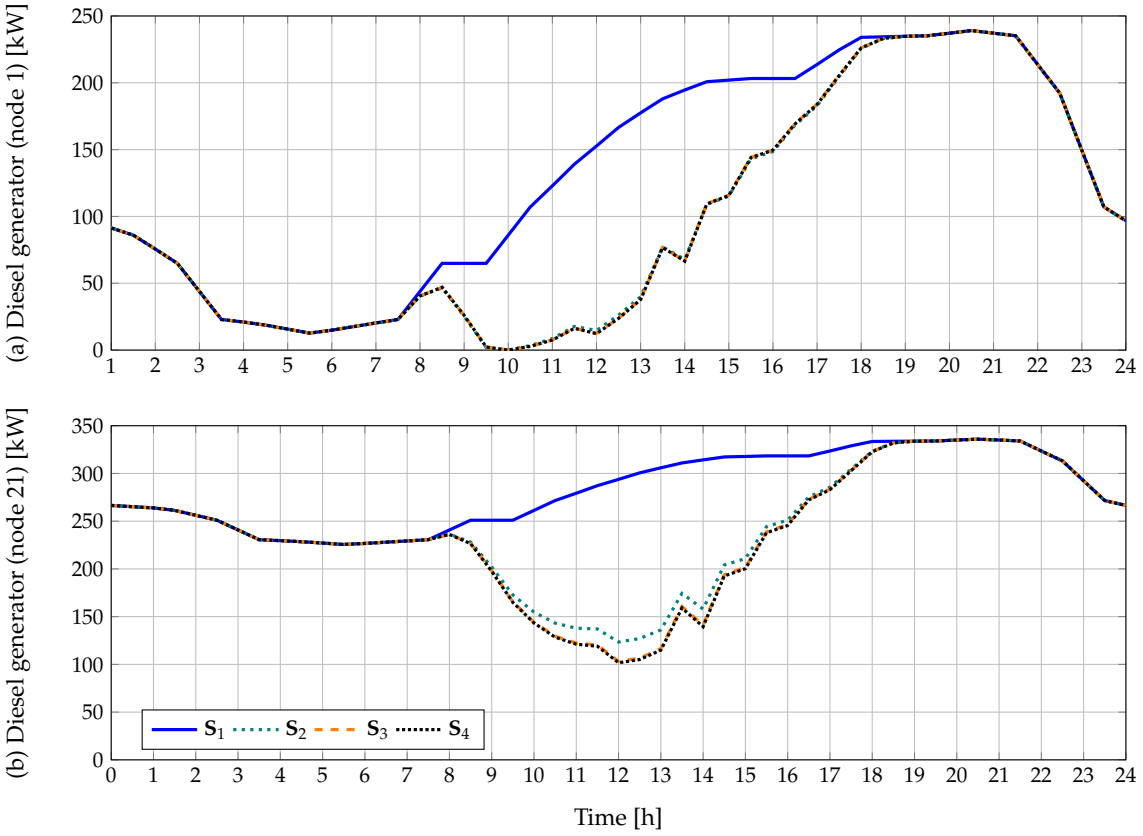

Figure 5. Generation profiles of the diesel sources during the day.

It is also important to mention that the differences between both profiles in the diesel generators are caused by the voltage profiles required at their terminals. In the case of the diesel generator located at node 21, it needs to inject more active power, since it is required to maintain the voltage at 1.05 p.u all the time, while the diesel generator located at node 1 was fixed to 1.0 p.u. This implies that with lower power injections this profile can be sustained.

6. Conclusions and Future Works

A mixed-integer nonlinear programming model for optimal location and sizing of PV sources in DC isolated networks was presented in this paper. The objective of this formulation is to reduce the total greenhouse emissions (i.e., pounds of CO_2 emissions per day) by diesel generators with the introduction of PV sources considering typical Colombian power profiles and consumption behaviors. Numerical results demonstrate that these gas emissions can be reduced between 17% and 19% depending on the number of PV sources installed and their sizes.

A nonlinear relation between the number of generators and their location was evidenced with the minimization of the objective function, as differences lower than 1.50% were found for all the scenarios that included PV sources (i.e., from the second to the fourth scenario). These situations imply that additional studies are needed in regard to operational costs, useful life and ground lot availability,

among other things, to determine the best solution in terms of PV sizes and locations. The objective function, in all scenarios provided in this studio, showed attractive alternatives to be implemented in the case of the 21-node test feeder.

As future work, it would be possible to extend this MINLP model to wind generators by predicting their average power availability with artificial neural networks with high efficiency, as reported in this study of PV sources. In addition, this model can be modified to include battery energy storage systems, to increase the introduction of renewable energy during periods of time with high demand and lower generation availability.

Author Contributions: Conceptualization, O.D.M., L.F.G.-N., W.G.-G., G.A. and Q.H.-E.; methodology, O.D.M., L.F.G.-N., W.G.-G., G.A. and Q.H.-E.; formal analysis, O.D.M., L.F.G.-N., W.G.-G., G.A. and Q.H.-E.; investigation, O.D.M., L.F.G.-N., W.G.-G., G.A. and Q.H.-E.; resources, O.D.M., L.F.G.-N., W.G.-G., G.A. and Q.H.-E.; writing—original draft preparation, O.D.M., L.F.G.-N., W.G.-G., G.A. and Q.H.-E. All authors have read and agreed to the published version of the manuscript.

Funding: This research was funded by the Universidad Tecnológica de Bolívar under project CP2019P011, and Instituto Tecnológico Metropolitano, Universidad Nacional de Colombia, and Colciencias under the project "Estrategia de transformación del sector energético Colombiano en el horizonte de 2030 - Energética 2030"—"Generación distribuida de energía eléctrica en Colombia a partir de energía solar y eólica" (Code: 58838, Hermes: 38945).

Conflicts of Interest: The authors declare no conflict of interest.

References

1. Blaabjerg, F.; Chen, Z.; Kjaer, S.B. Power electronics as efficient interface in dispersed power generation systems. *IEEE Trans. Power Electron.* **2004**, *19*, 1184–1194. [CrossRef]
2. Wandhare, R.G.; Agarwal, V. Novel Integration of a PV-Wind Energy System With Enhanced Efficiency. *IEEE Trans. Power Electron.* **2015**, *30*, 3638–3649. [CrossRef]
3. Montoya, O.D.; Gil-González, W.; Garces, A. Distributed energy resources integration in single-phase microgrids: An application of IDA-PBC and PI-PBC approaches. *Int. J. Electr. Power Energy Syst.* **2019**, *112*, 221–231. [CrossRef]
4. Gil-González, W.; Montoya, O.D.; Holguín, E.; Garces, A.; Grisales-Noreña, L.F. Economic dispatch of energy storage systems in dc microgrids employing a semidefinite programming model. *J. Energy Storage* **2019**, *21*, 1–8. [CrossRef]
5. Grisales, L.F.; Montoya, O.D.; Grajales, A.; Hincapie, R.A.; Granada, M. Optimal Planning and Operation of Distribution Systems Considering Distributed Energy Resources and Automatic Reclosers. *IEEE Lat. Am. Trans.* **2018**, *16*, 126–134. [CrossRef]
6. Montoya, O.D.; Grajales, A.; Garces, A.; Castro, C.A. Distribution Systems Operation Considering Energy Storage Devices and Distributed Generation. *IEEE Lat. Am. Trans.* **2017**, *15*, 890–900. [CrossRef]
7. Di Noia, L.P.; Genduso, F.; Miceli, R.; Rizzo, R. Optimal Integration of Hybrid Supercapacitor and IPT System for a Free-Catenary Tramway. *IEEE Trans. Ind. Appl.* **2019**, *55*, 794–801. [CrossRef]
8. Jayasinghe, S.D.G.; Vilathgamuwa, D.M.; Madawala, U.K. A Dual Inverter-Based Supercapacitor Direct Integration Scheme for Wind Energy Conversion Systems. *IEEE Trans. Ind. Appl.* **2013**, *49*, 1023–1030. [CrossRef]
9. Montoya, O.D.; Garcés, A.; Serra, F.M. DERs integration in microgrids using VSCs via proportional feedback linearization control: Supercapacitors and distributed generators. *J. Energy Storage* **2018**, *16*, 250–258. [CrossRef]
10. Gil-González, W.; Montoya, O.D.; Garces, A. Control of a SMES for mitigating subsynchronous oscillations in power systems: A PBC-PI approach. *J. Energy Storage* **2018**, *20*, 163–172. [CrossRef]
11. Shen, L.; Cheng, Q.; Cheng, Y.; Wei, L.; Wang, Y. Hierarchical control of DC micro-grid for photovoltaic EV charging station based on flywheel and battery energy storage system. *Electr. Power Syst. Res.* **2020**, *179*, 106079. [CrossRef]
12. Huang, C.N.; Chen, Y.S. Design of magnetic flywheel control for performance improvement of fuel cells used in vehicles. *Energy* **2017**, *118*, 840–852. [CrossRef]

13. Murad, M.A.A.; Milano, F. Modeling and Simulation of PI-Controllers Limiters for the Dynamic Analysis of VSC-Based Devices. *IEEE Trans. Power Syst.* **2019**, *34*, 3921–3930. [CrossRef]
14. Schiffer, J.; Seel, T.; Raisch, J.; Sezi, T. Voltage Stability and Reactive Power Sharing in Inverter-Based Microgrids With Consensus-Based Distributed Voltage Control. *IEEE Trans. Control Syst. Technol.* **2016**, *24*, 96–109. [CrossRef]
15. Joung, K.W.; Kim, T.; Park, J. Decoupled Frequency and Voltage Control for Stand-Alone Microgrid With High Renewable Penetration. *IEEE Trans. Ind. Appl.* **2019**, *55*, 122–133. [CrossRef]
16. Simpson-Porco, J.W.; Shafiee, Q.; Dörfler, F.; Vasquez, J.C.; Guerrero, J.M.; Bullo, F. Secondary Frequency and Voltage Control of Islanded Microgrids via Distributed Averaging. *IEEE Trans. Ind. Electron.* **2015**, *62*, 7025–7038. [CrossRef]
17. Garces, A. Uniqueness of the power flow solutions in low voltage direct current grids. *Electr. Power Syst. Res.* **2017**, *151*, 149–153. [CrossRef]
18. Montoya, O.D.; Gil-González, W.; Garces, A. Power flow approximation for DC networks with constant power loads via logarithmic transform of voltage magnitudes. *Electr. Power Syst. Res.* **2019**, *175*, 105887. [CrossRef]
19. Montoya, O.D.; Gil-González, W.; Garces, A. Optimal Power Flow on DC Microgrids: A Quadratic Convex Approximation. *IEEE Trans. Circuits Syst. II* **2019**, *66*, 1018–1022. [CrossRef]
20. Li, J.; Liu, F.; Wang, Z.; Low, S.H.; Mei, S. Optimal Power Flow in Stand-Alone DC Microgrids. *IEEE Trans. Power Syst.* **2018**, *33*, 5496–5506. [CrossRef]
21. Parhizi, S.; Lotfi, H.; Khodaei, A.; Bahramirad, S. State of the Art in Research on Microgrids: A Review. *IEEE Access* **2015**, *3*, 890–925. [CrossRef]
22. Montoya, O.D.; Gil-González, W.; Garces, A. Sequential quadratic programming models for solving the OPF problem in DC grids. *Electr. Power Syst. Res.* **2019**, *169*, 18–23. [CrossRef]
23. Montoya, O.D.; Gil-González, W.; Grisales-Noreña, L.F. Vortex Search Algorithm for Optimal Power Flow Analysis in DC Resistive Networks with CPLs. *IEEE Trans. Circuits Syst. II* **2019**. [CrossRef]
24. Garcés, A. On the Convergence of Newton's Method in Power Flow Studies for DC Microgrids. *IEEE Trans. Power Syst.* **2018**, *33*, 5770–5777. [CrossRef]
25. Montoya, O.D.; Garrido, V.M.; Gil-González, W.; Grisales-Noreña, L.F. Power Flow Analysis in DC Grids: Two Alternative Numerical Methods. *IEEE Trans. Circuits Syst. II* **2019**, *66*, 1865–1869. [CrossRef]
26. Yu, S.Y.; Kim, H.J.; Kim, J.H.; Han, B.M. SoC-Based Output Voltage Control for BESS with a Lithium-Ion Battery in a Stand-Alone DC Microgrid. *Energies* **2016**, *9*, 924. [CrossRef]
27. Robinson, S.; Papadopoulos, S.; Jadraque Gago, E.; Muneer, T. Feasibility Study of Integrating Renewable Energy Generation System in Sark Island to Reduce Energy Generation Cost and CO2 Emissions. *Energies* **2019**, *12*, 4722. [CrossRef]
28. Gil-González, W.; Montoya, O.D.; Garces, A. Modeling and control of a small hydro-power plant for a DC microgrid. *Electr. Power Syst. Res.* **2020**, *180*, 106104. [CrossRef]
29. Hassan, M.A.; Li, E.; Li, X.; Li, T.; Duan, C.; Chi, S. Adaptive Passivity-Based Control of dc–dc Buck Power Converter With Constant Power Load in DC Microgrid Systems. *IEEE J. Emerg. Sel. Top. Power Electron.* **2019**, *7*, 2029–2040. [CrossRef]
30. Shadmand, M.B.; Balog, R.S.; Abu-Rub, H. Model Predictive Control of PV Sources in a Smart DC Distribution System: Maximum Power Point Tracking and Droop Control. *IEEE Trans. Energy Convers.* **2014**, *29*, 913–921. [CrossRef]
31. Vafamand, N.; Khooban, M.H.; Dragičević, T.; Blaabjerg, F. Networked Fuzzy Predictive Control of Power Buffers for Dynamic Stabilization of DC Microgrids. *IEEE Trans. Ind. Electron.* **2019**, *66*, 1356–1362. [CrossRef]
32. Ghiasi, M.I.; Golkar, M.A.; Hajizadeh, A. Lyapunov Based-Distributed Fuzzy-Sliding Mode Control for Building Integrated-DC Microgrid With Plug-In Electric Vehicle. *IEEE Access* **2017**, *5*, 7746–7752. [CrossRef]
33. Mokhtar, M.; Marei, M.I.; El-Sattar, A.A. An Adaptive Droop Control Scheme for DC Microgrids Integrating Sliding Mode Voltage and Current Controlled Boost Converters. *IEEE Trans. Smart Grid* **2019**, *10*, 1685–1693. [CrossRef]
34. Liu, X.; Liu, Y.; Liu, J.; Xiang, Y.; Yuan, X. Optimal planning of AC-DC hybrid transmission and distributed energy resource system: Review and prospects. *CSEE J. Power Energy Syst.* **2019**, *5*, 409–422. [CrossRef]
35. Wogrin, S.; Gayme, D.F. Optimizing Storage Siting, Sizing, and Technology Portfolios in Transmission-Constrained Networks. *IEEE Trans. Power Syst.* **2015**, *30*, 3304–3313. [CrossRef]

36. Sachs, J.; Sawodny, O. A Two-Stage Model Predictive Control Strategy for Economic Diesel-PV-Battery Island Microgrid Operation in Rural Areas. *IEEE Trans. Sustain. Energy* **2016**, *7*, 903–913. [CrossRef]
37. Adefarati, T.; Bansal, R.C.; John Justo, J. Techno-economic analysis of a PV–wind–battery–diesel standalone power system in a remote area. *J. Eng.* **2017**, *2017*, 740–744. [CrossRef]
38. Moradi, M.; Abedini, M. A combination of genetic algorithm and particle swarm optimization for optimal DG location and sizing in distribution systems. *Int. J. Electr. Power Energy Syst.* **2012**, *34*, 66–74. [CrossRef]
39. Gandomkar, M.; Vakilian, M.; Ehsan, M. A Genetic–Based Tabu Search Algorithm for Optimal DG Allocation in Distribution Networks. *Electr. Power Components Syst.* **2005**, *33*, 1351–1362. [CrossRef]
40. Nekooei, K.; Farsangi, M.M.; Nezamabadi-Pour, H.; Lee, K.Y. An Improved Multi-Objective Harmony Search for Optimal Placement of DGs in Distribution Systems. *IEEE Trans. Smart Grid* **2013**, *4*, 557–567. [CrossRef]
41. Sultana, S.; Roy, P.K. Krill herd algorithm for optimal location of distributed generator in radial distribution system. *Appl. Soft Comput.* **2016**, *40*, 391–404. [CrossRef]
42. Grisales-Noreña, L.F.; Gonzalez Montoya, D.; Ramos-Paja, C.A. Optimal Sizing and Location of Distributed Generators Based on PBIL and PSO Techniques. *Energies* **2018**, *11*, 1018. [CrossRef]
43. Kaur, S.; Kumbhar, G.; Sharma, J. A MINLP technique for optimal placement of multiple DG units in distribution systems. *Int. J. Electr. Power Energy Syst.* **2014**, *63*, 609–617. [CrossRef]
44. Montoya, O.D.; Gil-González, W.; Grisales-Noreña, L. An exact MINLP model for optimal location and sizing of DGs in distribution networks: A general algebraic modeling system approach. *Ain Shams Eng. J.* **2019**. [CrossRef]
45. Montoya, O.D.; Gil-González, W.; Grisales-Noreña, L. Relaxed convex model for optimal location and sizing of DGs in DC grids using sequential quadratic programming and random hyperplane approaches. *Int. J. Electr. Power Energy Syst.* **2020**, *115*, 105442.[CrossRef]
46. Montoya, O.D. A convex OPF approximation for selecting the best candidate nodes for optimal location of power sources on DC resistive networks. *Eng. Sci. Technol. Int. J.* **2019**. [CrossRef]
47. Grisales-Noreña, L.F.; Garzon-Rivera, O.D.; Montoya, O.D.; Ramos-Paja, C.A. Hybrid Metaheuristic Optimization Methods for Optimal Location and Sizing DGs in DC Networks. In *Workshop on Engineering Applications*; Chapter Applied Computer Sciences in Engineering; Figueroa-García, J., Duarte-González, M., Jaramillo-Isaza, S., Orjuela-Cañon, A., Díaz-Gutierrez, Y., Eds.; Springer: Cham, Switzerland, 2019; Volume 1052, pp. 214–225. [CrossRef]
48. Montoya, O.D.; Garrido, V.M.; Grisales-Noreña, L.F.; Gil-González, W.; Garces, A.; Ramos-Paja, C.A. Optimal Location of DGs in DC Power Grids Using a MINLP Model Implemented in GAMS. In Proceedings of the 2018 IEEE 9th Power, Instrumentation and Measurement Meeting (EPIM), Salto, Uruguay, 14–16 November 2018; pp. 1–5. [CrossRef]
49. Maleki, A.; Pourfayaz, F.; Hafeznia, H.; Rosen, M.A. A novel framework for optimal photovoltaic size and location in remote areas using a hybrid method: A case study of eastern Iran. *Energy Convers. Manag.* **2017**, *153*, 129–143. [CrossRef]
50. Montoya, O.D.; Gil-González, W.; Grisales-Noreña, L.; Orozco-Henao, C.; Serra, F. Economic Dispatch of BESS and Renewable Generators in DC Microgrids Using Voltage-Dependent Load Models. *Energies* **2019**, *12*, 4494. [CrossRef]
51. Simpson-Porco, J.W.; Dörfler, F.; Bullo, F. On Resistive Networks of Constant-Power Devices. *IEEE Trans. Circuits Syst. II* **2015**, *62*, 811–815. [CrossRef]
52. Zhang, L. Artificial Neural Network Architecture Design for EEG Time Series Simulation Using Chaotic System. In Proceedings of the 2018 Joint 7th International Conference on Informatics, Electronics Vision (ICIEV) and 2018 2nd International Conference on Imaging, Vision Pattern Recognition (icIVPR), Kitakyushu, Japan, 25–29 June 2018; pp. 388–393. [CrossRef]
53. Du, Y.C.; Stephanus, A. Levenberg-Marquardt Neural Network Algorithm for Degree of Arteriovenous Fistula Stenosis Classification Using a Dual Optical Photoplethysmography Sensor. *Sensors* **2018**, *18*, 2322. [CrossRef]
54. Wilson, P.; Mantooth, H.A. Chapter 10—Model-Based Optimization Techniques. In *Model-Based Engineering for Complex Electronic Systems*; Wilson, P., Mantooth, H.A., Eds.; Newnes: Oxford, UK, 2013; pp. 347–367. [CrossRef]

55. Naghiloo, A.; Abbaspour, M.; Mohammadi-Ivatloo, B.; Bakhtari, K. GAMS based approach for optimal design and sizing of a pressure retarded osmosis power plant in Bahmanshir river of Iran. *Renew. Sustain. Energy Rev.* **2015**, *52*, 1559–1565. [CrossRef]
56. Montoya, O.D. Solving a Classical Optimization Problem Using GAMS Optimizer Package: Economic Dispatch Problem Implementation. *Ingenieria y Ciencia* **2017**, *13*, 39–63. [CrossRef]
57. GAMS Development Corp. GAMS Free Demo Version. Available online: https://www.gams.com/download/ (accessed on 14 February 2020).